IEEE Geoscience and Remote Sensing Letters, Volume 18, Issue 2, February 2021, pp. 266-270
DOI: 10.1109/LGRS.2020.2970249

# Characterisation of the internal structure of landmines using Ground Penetrating Radar

Federico Lombardi *Member, IEEE*, Hugh D. Griffiths, *Fellow, IEEE*, Maurizio Lualdi, and Alessio Balleri

***Abstract*— One of the principal limitations of employing Ground Penetrating Radar (GPR) for landmine detection is the presence of clutter, i.e. reflections from the surrounding environment which might interfere with the landmine echoes. Clutter presents similar scattering characteristics of typical targets and may significantly raise the detection threshold of the system. A capability to characterise the internal structure of a buried target might provide key unique information to develop advanced landmine-clutter discrimination algorithms, considering that the presence of internal scattering components can be univocally associated to man-made targets. In this paper, the possibility of identifying and characterising these contributions from the GPR signature of a landmine is numerically assessed and experimentally validated. The simulated response from a landmine-like target shows that the presence of the internal structure generates additional reflection peaks, as a consequence of the layered structure of the object, and the field trials corroborate that it is possible to identify these scattering components and delineate their spatial distribution.**

***Index Terms* — Ground Penetrating Radar, Landmine imaging, Radar image reconstruction, Trace positioning.**

## I. Introduction

Although, in recent years significant progress has been made on GPR for landmine detection [1], discriminating landmines from natural clutter remains a critical challenge [2], due to the wide possibility of clutter sources and soil temporal and spatial variability [3]. In this framework, understanding the electromagnetic signatures of landmines and identifying scattering features [4] that can uniquely define the nature of the target and unambiguously characterise a landmine can provide a stepchange in discrimination performance [5].

A common characteristic of cased man-made objects, including landmines, is the presence of a number of internal components that allow the device to function. A landmine, for example, can be modelled as a composite dielectric cylinder with a number layers that, when illuminated, produce multiple reflections which interfere to provide the overall target signature and Radar Cross Section (RCS) [6].

The vast majority of clutter targets are not hollow and therefore the detection of internal scattering components in the target radar signature can be unambiguously associated with a composite object. Consequently, a system capability to detect internal targets components might lead to the development of advanced classification algorithms and ultimately offer improved landmine-clutter discrimination performance [7].

In this paper, numerical simulations have been carried out to characterise the electromagnetic response of a modelled landmine-like target to investigate and demonstrate the effects of internal structure on the GPR signature. Experimental results from a field trial are then presented that validate the simulations and prove that the internal components could indeed be detected and properly characterised. The foreseen innovation is given by the fact that the investigated features are characteristic of the target itself and are not only source but also scenario independent, although the strength of the radar return may vary.

The paper is organised as follows: Section II presents the results from a numerical analysis to give a theoretical evidence of the variations in the target radar signature produced by the presence of the internal assemblies and to validate the research scope, while in Section III results from an experimental campaign are presented and discussed. Finally, conclusions are presented in Section IV.

## II. Landmine Radar Signature Characterisation

The possibility of properly identifying the reflections associated with the internal structure scattering in the landmine radar signature depends mainly on (1) the target scattering characteristics, as targets with different geometrical and/or physical properties will have a different RCS, and (2) the GPR range resolution, being the limit of certainty in distinguishing between two close scatterers.

To assess the impact of these two parameters, a number of numerical simulations have been carried out employing gprMax, an open-source FDTD solver available at http://www.gprmax.com [8].

The modelled environment consisted of a homogeneous sandy material hosting a target buried at a depth of 10 cm, value that recalls the requirement of the clearance programmes [9]. The source was a theoretical Hertzian dipole fed with a Ricker waveform

$$s(t) = (1 - 2\pi^2 f_0^2 \cdot t^2)\exp(-\pi^2 f_0^2 t^2) \quad (1)$$

The authors thank the Find A Better Way charity for their support of this research under the DETERMINE programme (grant number 2015/001D).

F. Lombardi and M. Lualdi are with the Department of Civil and Environmental Engineering, Politecnico di Milano, 20133 Milan. (e-mail: federico.lombardi@polimi.it, maurizio.lualdi@polimi.it).

H.D. Griffiths is with the Department of Electronic & Electrical Engineering, University College London, London, WC1E 6BT. (e-mail: h.griffiths@ucl.ac.uk).

A. Balleri is with the Centre for Electronic Warfare, Information and Cyber, Cranfield University, Defence Academy of the UK, Shrivenham, SN6 8LA. (email: a.balleri@cranfield.ac.uk)

with a central frequency ($f_0$) of 1.7 GHz and an approximate frequency band of 2 GHz [10].

The model parameters are detailed in Table I and Fig. 1.

TABLE I
NUMERICAL MODEL PARAMETERS

| Parameter | Value |
|---|---|
| Domain size | 50 x 80 cm |
| Spatial discretisation (dx, dy) | 0.1 – 0.05 cm |
| Time window | 12 ns |
| Time discretization | 0.0015 ns |
| Number of cells | $8 \cdot 10^5$ |
| Antenna separation | 6 cm |
| Antenna height | 1 cm |
| Central frequency | 1.7 GHz |
| Frequency span | 2 GHz |
| Soil dielectric ($\varepsilon_{soil}$) | 4.5 |
| Target depth | 10 cm |
| Target height | 6.5 cm |
| Target width | 8 cm |

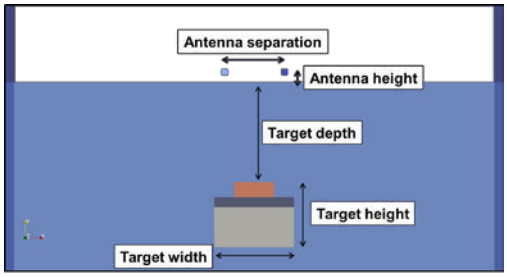

Fig. 1: gprMax modelled scenario and parameters indication.

The landmine-like object has been modelled as composed of:

- The activator pad (orange area in Fig. 1), characterised by a relative dielectric constant ($\varepsilon_{pad}$) of 7 and a thickness of 1.5 cm.
- An air layer ($\varepsilon_{air}$=1) representing the internal structure (dark grey area in Fig. 1) with a thickness of 1 cm.
- The main body of the mine (light grey area in Fig. 1), characterised by a relative dielectric constant ($\varepsilon_{expl}$) of 3 and a thickness of 4 cm.

From this simplified sketch, the radar signature is expected to produce three different contributions, even if the possibility of distinguishing each of them is to be verified.

As a general rule, two events can be distinguished if the targets are separated in time by a time difference at least equal to the -3 dB envelope width. The considered waveform exhibits a -3 dB envelope width of approximately 0.22 ns, resulting in a required time difference between the top and the bottom of each layer of 0.22 ns in order to be separated. To evaluate the expected discrimination performance, Table II specifies the temporal extension, given the material properties, of the previously described internal layers.

TABLE II
INTERNAL LAYERS CHARACTERISTICS

| Layer | Velocity | Temporal extension |
|---|---|---|
| Activator pad | 11.3 cm/ns | 0.13 ns |
| Air layer | 30 cm/ns | 0.03 s |
| Main body | 17.3 cm/ns | 0.24 ns |

From the table, it is inferable that the main body is the only contribution that could be correctly reconstructed, as the time separation between the top and the bottom of the layer is sufficiently wide. For the other two components, none of them are likely to be correctly reconstructed.

These considerations are described in Fig. 2, showing the computed analytical signal and the correspondent envelope together with the delayed version according to the temporal extension of each layer.

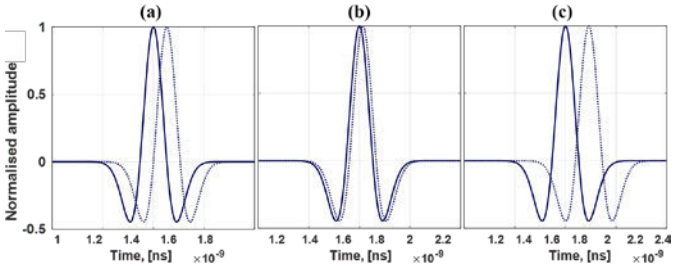

Fig. 2: MATLAB-simulated signals analysis: (a) activator pad. (b) air layer. (c) main body.

For a system with a flat frequency response, the pulse width equals the reciprocal of the bandwidth and the required bandwidth for the activator pad to be resolved is in the order of 4 GHz, while for the air layer, due to its high velocity of propagation and the reduced thickness, this value almost quadrupled. For most of the currently employed GPR systems, the trade-off between penetration and resolution has been solved by choosing a central frequency in the range 1 to 3 GHz, from which it follows that under realistic operating conditions, only a partial target reconstruction can be achieved.

Despite being theoretically independent from the surrounding soil characteristics, the ground additionally acts as a low-pass filter, placing a window across the antenna aperture and thus limiting the effective dominant wavelength of the signal.

Proceeding with the analysis of the target signature, Fig. 3 shows the gprMax simulated signatures of the activator pad and the air layer.

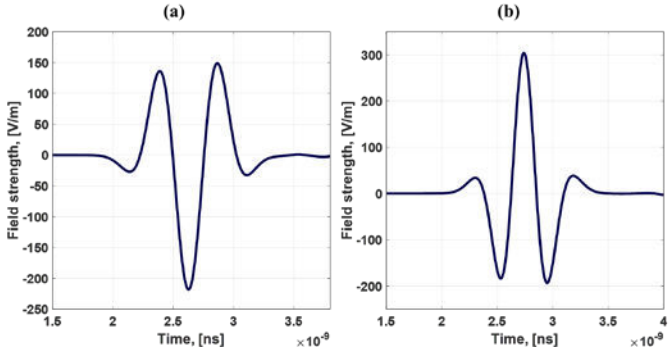

Fig. 3: Landmine-like object simulated response: (a) activator pad. (b) air layer

In accordance with the previous hypothesis, the contribution from the activator pad (Fig. 3a) is described by a single reflection event, exhibiting also a reverse in polarity due to a change in the reflection coefficient sign ($\varepsilon_{pad} > \varepsilon_{soil}$). The same behaviour, except for the polarity reversal, can be highlighted for the air layer contribution (Fig. 3b), similarly characterised by a regular scattering function.

The response from the main body, as shown in Fig. 4, exhibits two closely spaced events (marked A and B), belonging to the top and the bottom of the layer, both exhibiting a reversed polarity. In this case, the vertical extension of the layer is higher than the resolution limit and the layer can be properly reconstructed. In particular, the time peak-to-peak two way traveltime is approximately 0.45 ns, in agreement with the value in Table II, resulting in a computed layer thickness close to the specified one (4 cm).

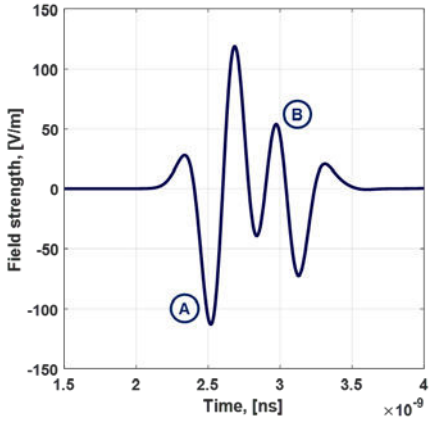


Fig. 4: Landmine-like object simulated response: main body component.

Finally, the effects of the mutual interference of the three layers due to their temporal succession needs to be addressed and, as in the previous analysis, the three contributions have been considered as separate events. Fig. 5 shows the temporal occurrence of the reflections events according to the internal geometry of the target.

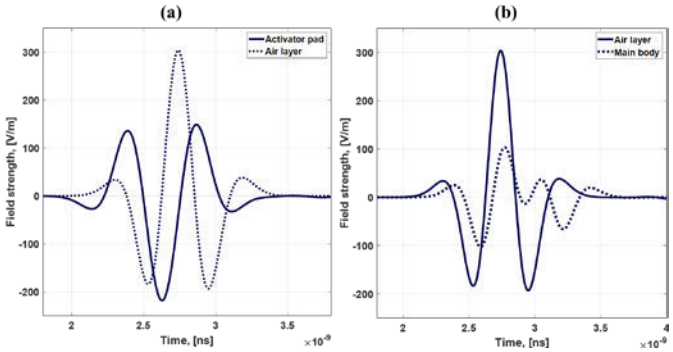


Fig. 5 Landmine-like object simulated temporal occurrence analysis: (a) activator pad and air layer component. (b) Air layer and main body component.

From Fig. 5a the interference between the reflections is expected to result in two well distinguishable peaks, given the location of the two signature components. On the contrary, the width of the air layer contribution (Fig. 5b) is likely to complete merge with the one generated by the main body, possibly limiting its detectability.

These considerations are confirmed when analysing the overall signature of the landmine-like target, shown in Fig. 6.

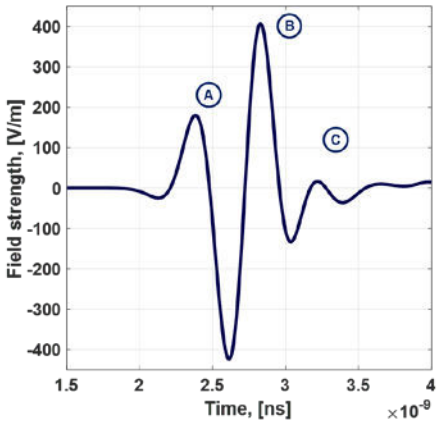


Fig. 6: Simulated response from a landmine-like target.

Consistently with Fig. 5, the three components lose their individual identity and hence prevent a straightforward reconstruction and interpretation of the result. However, the hypothesis of a heterogeneous target rather than a solid one can be supported by the fact that the signature is visibly asymmetric, both analysing the time separation of the peaks and their relative amplitudes. In particular, it is possible to safely identify three events: the top and the bottom reflections (respectively marked A and C in Fig. 6), and a sharp reflection (marked B in Fig. 6) occurring between these two, which can be associated with the scattering contribution produced by the internal air layer.

Therefore, a blind reconstruction of the target would lead to estimating the object as a composition of at least two different layers, the latter one characterised by a high dielectric contrast and a high velocity. A hint on the presence of a third layer can be made considering the peak-to-peak amplitude difference of the late reflections (marked B and C in Fig. 6), which might imply a reflections overlap, and the polarity outline of the latter one (marked C in Fig. 6).

As a final analysis, the comparison of the landmine-like target signature with the one generated by a solid homogeneous dielectric one, with the same dimensions and characterised by a dielectric constant ($\varepsilon_{solid}$) of 3, is provided in Fig. 7.

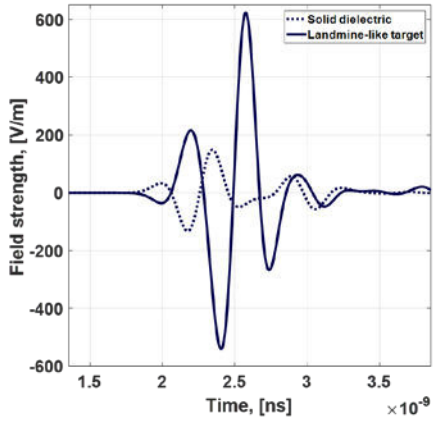


Fig. 7: Comparison between a landmine-like target and a homogeneous one.

The time separation of the top and the bottom of the homogeneous target (approximately 0.37 ns) is sufficient for the target to be reconstructed, and consequently its signature exhibits two reflections, spaced 0.36 ns and a stable behaviour between them. What can be additionally noticed is that the landmine-like target signature has a longer extension, in agreement with the presence of a faster medium.

In conclusion, it can be said that despite being partially under the resolution performance of the system, the object can be correctly identified as a composite target.

## III. Experimental Validation

The numerical analysis has been validated through a 3D field survey, employing a representative inert landmine model (pictured in Fig. 8) complete with all of its parts and filled with a high explosive simulant.


Fig. 8: Neutralised landmine. (a) External view. (b) Disassembled target [11]

The target was buried with the activator pad facing the surface at a depth of approximately 10 cm, in a sandy material characterised by a relative dielectric constant ($\varepsilon_{soil}$) of roughly 4.5. The GPR equipment employed for the measurements consisted of an IDS Aladdin radar (provided by IDS Georadar srl), an impulse device carrying dipole antennas separated by 6 cm with a central frequency and a bandwidth of 2 GHz.

Details of the field experimentation are provided in Table III.

TABLE III
FIELD ACQUISITION PARAMETERS

| Parameter | Value |
|---|---|
| Acquired area | 50 x 50 cm |
| Spatial sampling (dx, dy) | 0.4 – 0.8 cm |
| Time window | 20 ns |
| Time sampling | 0.0522 ns |
| Antenna separation | 6 cm |
| Antenna height | < 1 cm |
| Antenna frequency | 2 GHz |
| Antenna bandwidth | 2 GHz |
| Soil dielectric ($\varepsilon_{soil}$) | 4.5 |
| Target depth | 10 cm |
| Target height | 3.5 cm |
| Target width | 8.8 cm |

Except for a time calibration, performed through an autocorrelation function, and a frequency filtering to remove out of band noise, no additional processing steps have been applied on the data.

The acquired GPR signature of the target is presented in Fig. 9.

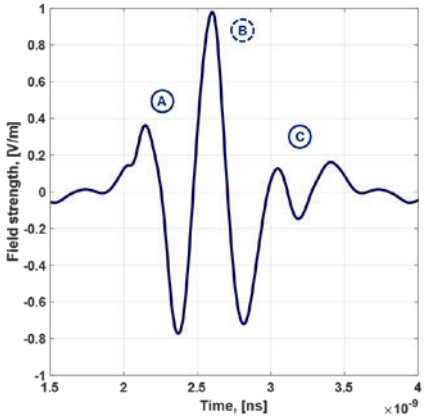


Fig. 9: Experimental response from a landmine-like target.

Three separate events can be identified, with a close correlation with the numerical results previously obtained and commented: the upper part of the landmine, a sharp reflection after it, and a weak response indicating the bottom of the target (respectively marked A, B, and C in Fig. 9), exhibiting a slightly more complex pattern probably due to the internal design of the target. Therefore, the internal structure contribution has confirmed to provide a reliable feature for identifying the target.

The results of the 3D analysis are presented in Fig. 10 and shown in terms of a set of time slices, i.e. the horizontal sections of the volume taken at specified time instant. The GPR slices are displayed in a blue-yellow-red colourmap and with normalised amplitude values.

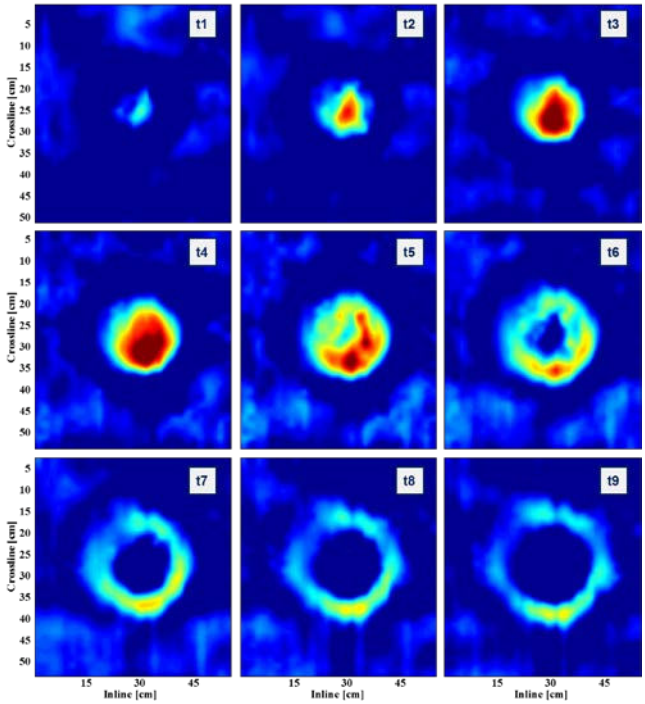


Fig. 10: SB-33 radar time slice. Order from left to right, top to bottom.

The results demonstrate the capability of GPR to delineate the internal structure reflections spatial distribution, thus providing enhanced information on the target.

In particular, the slice at *t4* shows a uniform high reflectivity area centred on the middle of the target, indicating a regular scattering element smaller than the target and located at its

centre. The hint on the contour of the feature arises from the fact that the maxima of the reflections are concentrated in a single location, with the amplitudes gradually decreasing following a hyperbolic behaviour. In the following slice (*t5*), the reflection distribution identifies a semi-circular shape, possibly generated by a number of scattering events near the outer border of the target. Also in this case, the extended element supposition, rather than a single point scatterer, comes from the analysis of the amplitude peaks pattern. The target contribution in the subsequent slices (*t6* onward) is reduced due to the effect of the highly reflective layer.

In conclusion, the internal structure of the target can be considered consisting of a regular central element and a high scattering region covering only a part of it.

The imaging performance can be better evaluated by overlaying the radar results with the landmine cutaway, as provided in Fig. 11, in which the correspondence between the actual design and the supposed structure is plainly visible.

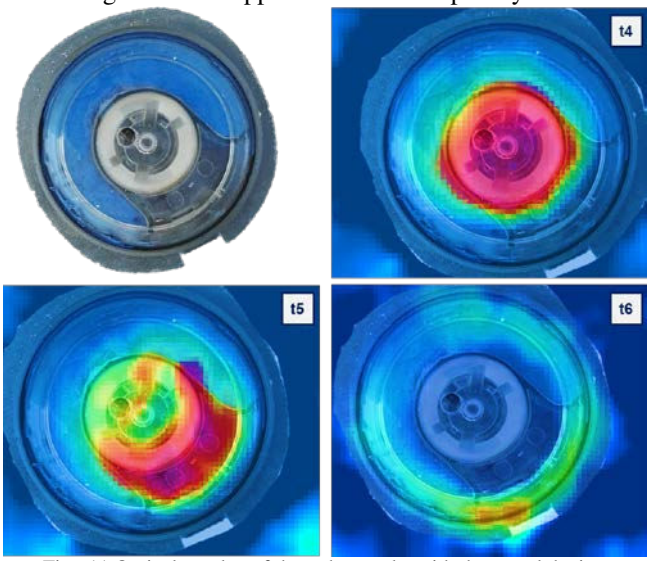

Fig. 11 Optical overlay of the radar results with the actual device.

The central scattering feature highlighted in the radar slice *t4* is confirmed to be the fuse and striker assembly, which has a regular cylindrical shape. The radar anomaly marked *t5*, instead, appears compatible with the void area of the landmine, positioned aside of the fuse and encompassing it, both in terms of location and shape. This validates also the absence of data in the successive slices.

Finally, the overlay provides also a further correspondence for the circular evidence (*t6*): superimposing the two images, one can note that the bolder part represents the detonator capsules signature.

## IV. Conclusion

The possibility of characterising the internal structure of a buried target from its radar images might represent a significant achievement for increasing the performance and efficiency of GPR for landmine detection.

The outcomes of the research have demonstrated that, despite the limited thickness of its assemblies, which means that only a partial reconstruction is achievable due to resolution limits, the internal structure of a landmine does have a noticeable effect on the target signature, both in ideal and more realistic conditions.

In addition, the GPR slices showed that the internal structure can be geometrically delineated and reconstructed with a very close correspondence with the actual physical structure.

Ongoing developments are focussed on determining the robustness of the approach, both in terms of GPR system configuration and target characteristics reliance. First of all, the experiment and the simulations were all carried out considering proximal operations, i.e. a limited antenna-ground surface separation, to maximise the energy coupling process and consequently the target scattering contribution. Progressively elevating the source from the ground is expected to alter the pattern of the landmine signature and potentially lead to a reduction in detection performance. Therefore, a further investigation to quantify these effects is needed, considering also the potential advantage of operating the system at a stand-off distance. Other key parameters that are currently researched are the impact on the landmine structure detectability of a change in the target inclination angle and its burial depth.

## Acknowledgment

The authors thank the Defence Academy Ammunition Hall for providing the landmines used for the experimental measurements.

## References

[1] D. J. Daniels, "An assessment of the fundamental performance of GPR against buried landmines," Proc. SPIE 6553, Detec. Rem. Technol. for Mines and Minelike Targets XII, vol. 6553, 65530G, May 2007. 10.1117/12.715142.

[2] A. Genc, G.B. Akar, "Combination of physics-based and image-based features for landmine identification in ground penetrating radar data," *J. Appl. Rem. Sens.* vol. 13, no. 2, pp. 026503, Apr. 2019, 10.1117/1.JRS.13.026503

[3] X. Núñez-Nieto, M. Solla, P. Gómez-Pérez, and H. Lorenzo, "GPR signal characterization for automated landmine and UXO detection based on machine learning techniques". *Remote sensing*, vol. 6, no. 10, pp. 9729-9748, 2014.

[4] C. R. Ratto, P. A. Torrione and L. M. Collins, "Exploiting Ground-Penetrating Radar Phenomenology in a Context-Dependent Framework for Landmine Detection and Discrimination," *IEEE Trans. Geosci. Remote Sens.*, vol. 49, no. 5, pp. 1689-1700, May 2011. 10.1109/TGRS.2010.2084093

[5] O. Lopera, N. Milisavljevie, D. Daniels and B. Macq, "Time-frequency domain signature analysis of GPR data for landmine identification," in Proc. 4th Int. Workshop Adv. GPR, Naples, Italy, Jun 2007, pp. 159-162. 10. 1109/AGPR.2007.386544

[6] Lombardi, F., Griffiths, H.D., Wright, L., Balleri, A.: 'Dependence of landmine radar signature on aspect angle', *IET Radar, Sonar Nav.*, vol. 11, no. 6, pp. 892 – 902, Jun 2017, 10.1049/iet-rsn.2016.0491.

[7] Lombardi, F., Griffiths, H.D., Balleri, A.: 'Landmine internal structure detection from Ground Penetrating Radar images', IEEE Radar Conf., Oklahoma City, USA, April 2018, pp. 1201-1206. 10.1109/RADAR.2018.8378733

[8] Warren, C., Giannopoulos, A., Giannakis I.: 'gprMax: Open source software to simulate electromagnetic wave propagation for Ground Penetrating Radar', Comp. Phys. Comm., 2016, vol. 209, pp. 163-170. 10.1016/j.cpc.2016.08.020

[9] International Standards for Humanitarian Mine Clearance Operations. http://www:un:org/Depts/mine/Standard/glossary:htm.

[10] Wang, Y.: 'Frequencies of the Ricker wavelet'. Geophysics, 2015, vol. 80, n. 2, pp. A31-A37. 10.1190/GEO2014-0441.1

[11] Ressler, D., 'Study of the Effects of Aging on Landmines' (2010). CISR Studies and Reports. http://commons.lib.jmu.edu/cisr-studiesreports/1